Ellipsometric studies of $Be_xZn_{1-x}Se$ between 3 eV and 25 eV

K. Wilmers* and T. Wethkamp
Institut für Festkörperphysik, TU Berlin, Hardenbergstrasse 36, D-10623 Berlin, Germany
and Max-Planck-Institut für Festkörperforschung, Heisenbergstrasse 1, D-70569 Stuttgart, Germany

N. Esser, C. Cobet, and W. Richter
Institut für Festkörperphysik, TU Berlin, Hardenbergstrasse 36, D-10623 Berlin, Germany

M. Cardona
Max-Planck-Institut für Festkörperforschung, Heisenbergstrasse 1, D-70569 Stuttgart, Germany

V. Wagner, H. Lugauer, F. Fischer, T. Gerhard, and M. Keim
Physikalisches Institut, Universität Würzburg, Am Hubland, D-97074 Würzburg, Germany
(Received 27 August 1998)

We have determined the dielectric function of $Be_xZn_{1-x}Se$ above the fundamental absorption edge for the full composition range ($0 \leqslant x \leqslant 1$) by spectroscopic ellipsometry in the UV and VUV range. The spectra show pronounced features in the photon energy range between 2.7 and 25 eV. By comparing the ZnSe spectra ($x=0$) to literature data, we assign the observed structures to interband transitions at specific points or regions of the Brillouin zone. The corresponding assignment for BeSe is made by tracking the systematic dependence of these structures on the Be content x from $x=0$ to $x=1$. E_0 has the steepest slope dE_0/dx and exhibits a bowing vs x. On samples with a large Zn content ($x<0.2$) two structures show up at high energies (15.7 and 16.9 eV) which have not been observed before. We assign these structures to transitions from the Zn $3d$ bands to a higher conduction band at the L point and at the Γ point. [S0163-1829(99)01515-5]

I. INTRODUCTION

Devices based on II-VI semiconductors, such as ZnSe laser diodes, have a reduced lifetime compared to III-V based devices due to defect formation favored by the high ionicity and the smaller bond energies of conventional II-VI materials. Recently, however, it has been demonstrated that Be-VI compounds have a high degree of covalent bonding and bond energies similar to GaN.[1] This should entail a lattice hardening and slower degradation with time.

Therefore, II-VI compounds containing beryllium have become interesting materials for optoelectronic devices like green and blue laser diodes.[1–5] For instance, quarternary compounds, such as $Be_xMg_yZn_{1-x-y}Se/GaAs(001)$, may be used to tailor the optical and electronic properties over a wide range by varying the composition (x,y) under conditions of lattice matching to GaAs.[1,2]

Beryllium chalcogenides, however, are a rather new class of materials; their optical and electronic properties have not yet been elucidated. As we show below, BeSe has a fundamental band gap of 5.5 eV while the band gap of ZnSe is 2.7 eV. Thus, by varying the stoichiometry in $Be_xZn_{1-x}Se$ a wide range of band-gap energies is covered and even small differences of the beryllium content in alloys cause large band-gap shifts.

The technique of spectroscopic ellipsometry is well established for investigating the optical properties of bulk materials and thin films.[6,7] It facilitates the direct determination of the complex dielectric function $\epsilon = \epsilon_1 + i\epsilon_2$ and thus circumvents the need for a Kramers-Kronig transformation. ϵ is directly related to the electronic band structure of the material through interband transitions. Wide band-gap materials exhibit their main interband transitions within the spectral range from 3 to 15 eV, i.e., in the UV/VUV spectral region. Since this range is not fully accessible to conventional ellipsometers, which are limited to approximately 6 eV, we used the VUV ellipsometer at BESSY in the range of 2.5 to 25 eV with a synchrotron radiation source.

Various $Be_xZn_{1-x}Se$ samples with different beryllium contents were investigated at room temperature. The results obtained for the two binary compounds ZnSe and BeSe were compared to band-structure calculations and dielectric functions derived therefrom. We compared reflectivity data available in the literature for ZnSe to the reflectivity calculated from our ellipsometry measurements.

No experimental data in the VUV spectral range were previously available for the beryllium containing alloys. Local-density approximation density-functional theory (LDA-DFT) calculations for BeSe (Ref. 8) predict that, in contrast to ZnSe, the interband transition at the L point from the top valence band to the lowest conduction band has a higher energy than that at the X point. Our experimental data for BeSe do not allow for an unambiguous interpretation of structures in ϵ because the main structures of the BeSe dielectric function appear very close to each other in energy, and thus are difficult to resolve. In this article, however, we show that an assignment of spectral features becomes possible when tracking the evolution of the dielectric function with varying x.

II. EXPERIMENTAL DETAILS

The experiments were carried out with the VUV ellipsometer at the 2m-Seya-Namioka beamline at BESSY. High in-

tensity, natural collimation, and the high degree of linear polarization of synchrotron radiation are essential for ellipsometric measurements. The accessible spectral range of the 2m-Seya-Namioka beamline is 2.5 to 35 eV.

The VUV ellipsometer operates with two different rotating analyzers. Below 10 eV, we use MgF_2 Rochon prisms as polarizer and rotating analyzer. Above 10 eV there are no transparent, birefringent materials that could be used as polarizers or analyzers. That is why we use the reflection near the pseudo-Brewster angle to polarize the light; i.e., a fixed configuration of three reflecting gold surfaces constitutes the rotating analyzer. Since this is not an ideal polarizer, numerical corrections must be applied to the measured data above 10 eV.[9,10] The two different analyzers are attached to the main UHV chamber in two separate chambers at different angles of incidence, $\Phi = 67.5°$ and $\Phi = 45°$, respectively.

Up to 10 eV the VUV ellipsometer has the same accuracy as a conventional one with light sources limited to 6 eV.[11] Above 10 eV, however, we find the polarization nonidealities mentioned above. Furthermore, a significant contribution effected by second-order diffracted light between approximately 10 and 13 eV (i.e., 20 to 26 eV photon energies) shows up in the spectra presented here. Between 10 and 13 eV, this causes a reduced amplitude in ϵ_2 and an artificial broad structure in ϵ_1. Moreover, diffuse scattered light coming from the zero order of the monochromator grating gives rise to a feature between 10 and 11 eV. As a consequence, the absolute values of the dielectric function are not reliable between 10 and 13 eV. A more detailed description of the experimental setup is given in the Refs. 9–11.

The investigated $Be_xZn_{1-x}Se$ layers were grown on GaAs in a Riber 2300 four-chamber MBE-system. First, homoepitaxial buffer layers were grown on GaAs substrates. Elemental Be, Se, and Zn effusion cells were employed for $Be_xZn_{1-x}Se$ layer growth. Usually, a substrate temperature of 300 °C was chosen. Composition and strain of the samples were determined by high-resolution x-ray diffraction. Layers with a Be content larger than $x = 0.2$ were found to be relaxed (i.e., not pseudomorphic). The samples (004) reflex width vary between 150'' and 850'' full width at half maximum (GaAs substrate: 17''–38''). Layer thickness ranges between 200 and 800 nm, exceeding the penetration depth of light above the fundamental bandgap. The samples were transported from the molecular-beam epitaxy chamber to the UHV chamber of the VUV ellipsometer in a nitrogen atmosphere in order to avoid contamination or oxidation.

III. RESULTS AND DISCUSSION

A. ZnSe

The experimentally determined pseudo-dielectric function $\langle \epsilon \rangle$ and the resulting reflectivity R of ZnSe are plotted in Fig. 1. Most of the features are well known from previous work.[12–19] Table I displays the calculated critical point energies from Ref. 18 and those of the structures we find in our ellipsometric spectra. In these spectra Fabry-Perot interferences dominate up to 2.69(1) eV, where the absorption at the fundamental band gap E_0 sets in. The imaginary part $\langle \epsilon_2 \rangle$ of the pseudodielectric function shows two strong maxima, one at 4.77(1) eV (E_1) with a shoulder at 5.04(1) eV ($E_1+\Delta_1$) and the second one at 6.25(1) eV (E_2). A weaker maximum

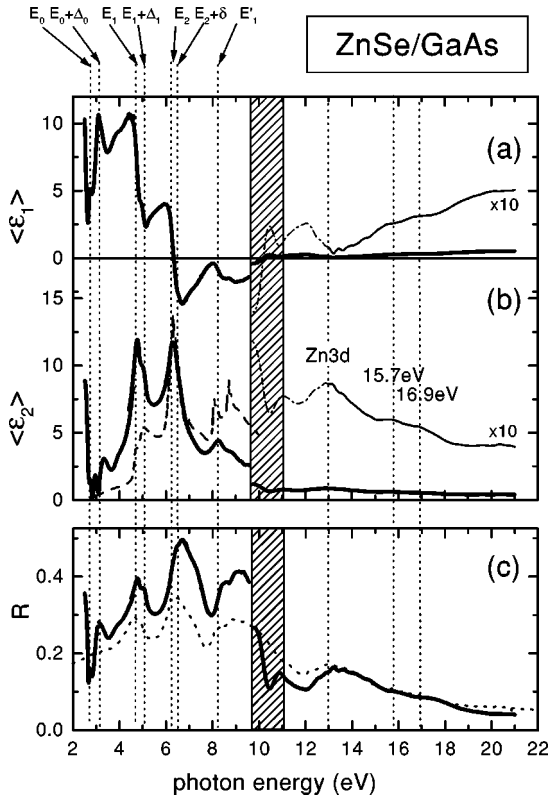

FIG. 1. Real part $\langle \epsilon_1 \rangle$ (a) and imaginary part $\langle \epsilon_2 \rangle$ (b) of the pseudodielectric function (Ref. 30) and the reflectivity R (c) of ZnSe. The solid curves display our data, the thin curves present these data scaled vertically by a factor 10. Stray light dominates the measured signal in the hatched section between 10 and 11 eV. Between 10 and 13 eV, the reduction in $\langle \epsilon_2 \rangle$ and the broad peak in $\langle \epsilon_1 \rangle$ are due to second-order light effects (dashed segment) (see experimental details). The dashed curve in (b) is the imaginary part of the dielectric function as derived from LDA-DFT band-structure calculations (Ref. 17). In (c) the reflectivity calculated from the ellipsometric data is shown as a solid curve, the dotted curve reproduces the reflectivity reported in Ref. 16.

is observed at 8.27(2) eV (E_1'). In the high-energy regime a broad structure appears at around 13 eV. This structure is assigned to transitions from the Zn $3d$ bands to the lowest conduction band,[16] which are resolved into three peaks in second derivatives of the spectra. In addition to these Zn $3d$ transitions at 12.34(5), 12.84(5), and 13.15(5) eV (from Zn $3d$ to Γ_6^c, L_6^c, and X_6^c, respectively, see Table I) we observe structures at 15.7(1) and 16.9(1) eV, which have not been reported in relevant publications to our knowledge. We assign these structures to Zn $3d$ transitions to higher conduction bands. Localizing the Zn $3d$ band 9 eV below the valence band edge[18] (9 eV is the value determined by photoemission[20–22]), we find corresponding gap energies of 16.3 and 16.4 eV (Zn $3d \rightarrow \Gamma_7^c, \Gamma_8^c$) at the center of the Brillouin zone as well as 16.7 eV (Zn $3d \rightarrow L_6^c$, $L_{4,5}^c$) at the L point (see Table I).

The imaginary part of the dielectric function as derived from pseudopotential band structure calculations[17] [dashed curve in Fig. 1(b)] and our measurement show a good overall agreement of peak positions; this agreement improves slightly at lower energies (see Table I). The amplitude of the structures is underestimated at lower energies and overesti-

TABLE I. Location in the Brillouin zone, symmetry, and energy of the calculated interband critical points for ZnSe (from Ref. 18) and energies of the corresponding structures observed for ZnSe and BeSe by means of ellipsometry.

After Ref. 19	Location in the Brillouin zone	Symmetry	Critical-point energy (eV)	Ellipsometry structure (eV)	
		Calculated for ZnSe[18]		ZnSe	BeSe
E_0	$\Gamma_8^v-\Gamma_6^c$	M_0	2.77	2.69(1)	5.55(1)
$E_0+\Delta_0$	$\Gamma_7^v-\Gamma_6^c$	M_0	3.22	3.11(1)	5.8(1) [a]
E_1	$L_{4,5}^v-L_6^c$ (0.5,0.5,0.5)	M_1	4.72	4.77(1)	6.15(1)
$E_1+\Delta_1$	$L_6^v-L_6^c$	M_1	5.00	5.04(1)	6.30(1)
E_2	$\Delta_5^v-\Delta_5^c$ (0.5,0.0,0.0)	M_0	6.55	6.25(1)	6.56(1)
$E_2+\delta$	$\Delta_5^v-\Delta_5^c$ (0.6,0.0,0.0)	M_1	7.08	6.62(1)	
E_0'	$\Gamma_8^v-\Gamma_8^c$ (0.0,0.0,0.0)	M_0	7.42	7.25(5)	7.29(1)
$E_0'+\Delta_0$	$\Gamma_7^v-\Gamma_6^c$	M_0	7.87		
E_1'	$L_{4,5}^v-L_{4,5}^c,L_6^c$ (0.5,0.5,0.5)	M_0	8.46	8.27(2)	8.47(2)
	$\Lambda_{4,5}^v-\Lambda_{4,5},\Lambda_6^c$ (0.35,0.35,0.35)	M_1	8.48		
$E_1'+\Delta_1$	$L_6^v-L_{4,5},L_6^c$ (0.5,0.5,0.5)	M_0	8.74		
	$\Lambda_6^v-\Lambda_{4,5},\Lambda_6^c$ (0.35,0.35,0.35)	M_1	8.76		
	Zn $3d$-Γ_6^c		11.76	12.34(5)	
	Zn $3d$-L_6^c		12.96	12.84(5)	
	Zn $3d$-X_6^c		13.54	13.15(5)	
	Zn $3d$-Γ_7^c		16.33	15.7(1)	
	Zn $3d$-Γ_8^c		16.42		
	Zn $3d$-L_6^c		16.68	16.9(1)	
	Zn $3d$-$L_{4,5}^c$		16.72		

[a]Value derived from a fit to the measured values of $E_0+\Delta_0(x)$.

mated at higher energies, a well-known observation usually attributed to excitonic effects in the calculations.[23,24]

The reflectivity was calculated from the ellipsometric data for comparison with the reflectivity measurement made on a cleaved ZnSe sample[16] [dotted curve in Fig. 1(c)]. The peak positions observed in the measured reflectivity are in excellent agreement with the normal incidence reflectivity calculated from our data. Also the absolute values are the same at high energies. Below 10 eV, however, the VUV ellipsometer yields significantly higher reflectivity, probably due to a higher accuracy of the ellipsometric experiment or more favorable surface preparation. The structure between 10 and 11 eV results from the artifact of the spectrometer mentioned above.

B. BeSe

Figure 2 shows similar spectra for BeSe. In the transparent regime up to 5.5 eV Fabry-Perot interferences also dominate the measured pseudodielectric function. Above 5.5 eV, the imaginary part of the dielectric function increases to a strong maximum at 6.5 eV followed by a decrease with weak superimposed structures. This indicates that the direct band gap E_0 is situated at 5.5 eV.

The band-structure calculation [density-functional theory, local-density approximation (LDA-DFT) scalar relativistic pseudopotential without spin-orbit splitting] underlying the calculated dielectric function[8] predicts that BeSe is an indirect band-gap semiconductor ($\Gamma\rightarrow X$). For this material the top valence and the lowest conduction bands are nearly parallel along L–Γ–X. The calculated gap energy between these two bands is 4.5 eV at the Γ point (E_0), i.e., 1 eV below the measured absorption edge at 5.5 eV in our ellipsometry spectrum. This fact must be a reflection of the so-called gap problem associated with the LDA approach to exchange and correlation.[25,26] In contrast to ZnSe (6.5 eV at X and 4.72 eV at L),[17] the gap energy between the top valence band and the lowest conduction band is smaller at the X point (5.1 eV) than at the L point (5.3 eV).

The dielectric function derived from this band-structure calculation is very similar in line shape to the experimental results, but the positions of the features are shifted to lower energies: the absorption edge appears at 4.5 eV and the maximum at 6 eV, i.e., 1 eV and 0.5 eV below the experimental features, respectively. A small absorption below E_0 is observed in the ellipsometry spectra, corresponding to the indirect gap found in the calculated band structure.

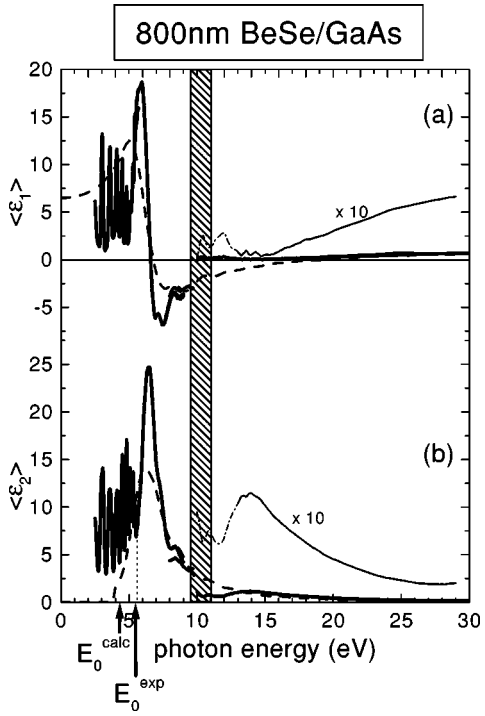

FIG. 2. Real part $\langle \epsilon_1 \rangle$ (a) and imaginary part $\langle \epsilon_2 \rangle$ (b) of the pseudodielectric function (Ref. 30) of BeSe. The solid curves show the measured pseudodielectric function; the dielectric function as derived from LDA-DFT band structure calculations (Ref. 8 is shown by dashed lines. The thin curves represent our experimental results scaled vertically by a factor 10. Stray light dominates the measured signal in the hatched section between 10 and 11 eV. Between 10 and 13 eV, the reduction in $\langle \epsilon_2 \rangle$ and the broad peak in $\langle \epsilon_1 \rangle$ are due to second-order light effects (dashed segment) (see experimental details).

The assignment of the structures in the BeSe spectra is difficult because they appear in a very small energy range and are therefore not resolved. This problem can be overcome by investigating the composition dependence of the structures observed in the mixed crystals $Be_xZn_{1-x}Se$ $[E_{cp}(x)]$.

C. $Be_xZn_{1-x}Se$

The spectra of $Be_xZn_{1-x}Se$ (Fig. 3) show a clear composition dependence for most of their structures. The structures are reduced in amplitude and broadened in the composition range around $x=0.5$, similar to what is known for other ternary alloy systems (see e.g., Ref. 11). A more detailed analysis based upon the second derivatives of the spectra leads to the diagram shown in Fig. 4.

The structures assigned to E_0, $E_0+\Delta_0$, E_1, $E_1+\Delta_1$, E_2, E_0', and E_1' in ZnSe are observed in all of the samples and with increasing beryllium content their spectral positions systematically shift towards higher energies. The critical points show different slopes dE/dx, E_0, and $E_0+\Delta_0$ having the steepest slope and show a bowing that is known for most ternary semiconductor mixed crystals.[27] The bowing parameter $b=1.1(1)$ eV for E_0 and $E_0+\Delta_0$, $b=0.8(1)$ eV for E_1, and $b=0.6(1)$ eV for $E_1+\Delta_1\{E(x)=E(0)+[E(1)-E(0)]\times x+b\times x\times(x-1)\}$. The energy separation of the E_1 and E_2 transitions decreases with increasing Be content from 1.5 eV in ZnSe to 0.4 eV in BeSe, but there is clearly no crossing of these gaps as the calculated band structure predicts[8] (see BeSe: in contrast to ZnSe, for BeSe the calculated gap energy at the X point is smaller than the one at the L point).

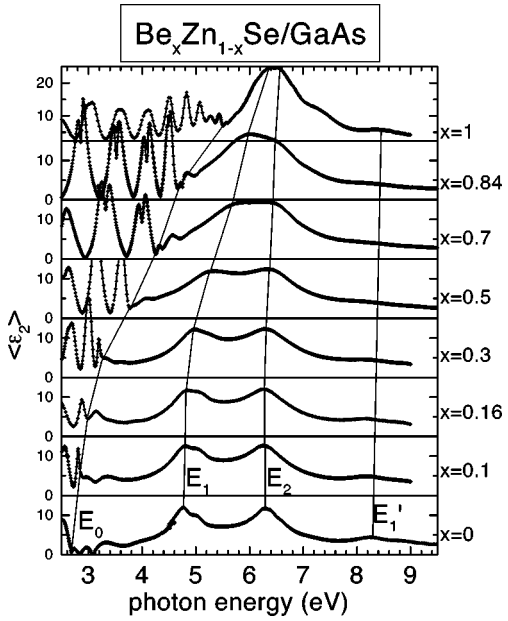

FIG. 3. The imaginary part $\langle \epsilon_2 \rangle$ of the pseudodielectric function (Ref. 30) for eight $Be_xZn_{1-x}Se$ samples with different compositions. The beryllium content x is indicated for each spectrum. The thin lines mark the positions of the main structures.

The valence-band spin-orbit splitting at the zone center Δ_0 is 0.42(2) for ZnSe, while for BeSe $\Delta_0=0.25(10)$ is significantly smaller. This might be due to the fact that the hybride covalency (see Ref. 1) of BeSe is larger (0.79) than

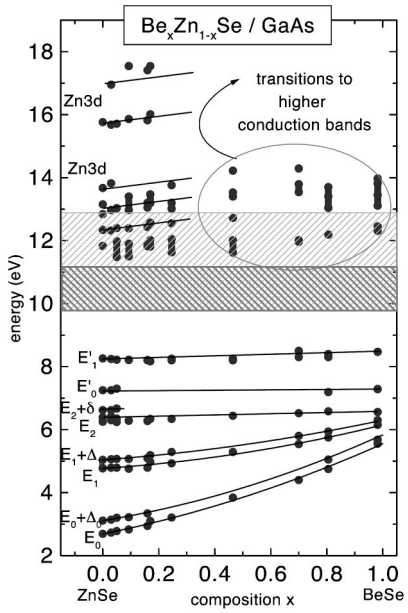

FIG. 4. The critical energies of the observed structures as a function of the composition. Stray light dominates the measured signal in the hatched section between 10 and 11 eV. Between 10 and 13 eV, second-order light influences the spectra (see experimental details).

that of ZnSe (0.66).[1] This should result in a more important contribution of the atomic spin-orbit splitting of Be ($\simeq 0$) to Δ_0 and Δ_1. For ZnSe, the ratio between Δ_0 and the valence-band spin-orbit splitting in the $\langle 111 \rangle$ direction (Δ_1) Δ_0/Δ_1 is about 1.5(1), for BeSe Δ_0/Δ_1 is about 1.6(1). This is the standard situation in most tetrahedrally coordinated semiconductors.[28]

The assignment of the observed structures in BeSe and ZnSe to interband transitions is displayed in Table I. Additional structures in the higher energy regime are observed at 11–14 eV for all compositions, i.e., they are not related to the Zn content. The structure at 12 eV could possibly be attributed to the second-order light contribution (see experimental details). Most likely, however, it is related to the samples since no features appear in the spectra above 20 eV. The Se $3d$ states are located 59 eV below the conduction band[29] and therefore do not cause any structures within our experimental spectral range. The inspection of the calculated BeSe band structure[8] reveals that the corresponding interband transitions cannot result from transitions of the *s*-like (lower) valence band into the lowest conduction band. We therefore conjecture that these structures come from transitions from the *p*-like (upper) valence bands to higher conduction bands.

IV. CONCLUSION

The dielectric function of $Be_xZn_{1-x}Se$ mixed crystals has been determined as a function of x in the VUV spectral range. The energies found for the optical gaps of ZnSe agree well with previously published data. In addition to the transitions from Zn $3d$ to the lowest conduction band at 12.34, 12.84, and 13.15 eV we observe structures at 15.7 and 16.9 eV, which we assign to Zn $3d$ transitions to higher conduction bands. The spectral structures in the dielectric function of BeSe were interpreted by investigating the ternary system $Be_xZn_{1-x}Se$. The lowest direct gap E_0 of BeSe has an energy of 5.5 eV. We assign the structures observed between 13 and 14 eV to transitions from the top valence bands to higher conduction bands.

ACKNOWLEDGMENTS

We greatly appreciate the support of Dr. F. Fleszar, especially for supplying band-structure and dielectric function calculations of BeSe prior to publication. We would like to acknowledge financial support from the BMBF under 05 622 ESA 2.

*Author to whom correspondence should be addressed. FAX: ++49-30-314-21769. Electronic address: katrin.wilmers@physik.tu-berlin.de

[1] G. Landwehr, F. Fischer, T. Baron, T. Litz, A. Waag, K. Schüll, H. Lugauer, T. Gerhard, M. Keim, and U. Lunz, Phys. Status Solidi B **202**, 645 (1997).

[2] A. Waag, F. Fischer, H.-J. Lugauer, Th. Litz, T. Gerhard, J. Nürnberger, U. Lunz, U. Zehnder, W. Ossau, G. Landwehr, B. Roos, and H. Richter, Mater. Sci. Eng., B **43**, 65 (1997).

[3] Th. Litz, H. J. Lugauer, F. Fischer, U. Zehnder, U. Lunz, Th. Gerhard, H. Ress, A. Waag, G. Landwehr, Mater. Sci. Eng., B **43**, 83 (1997).

[4] A. Waag, F. Fischer, K. Schull, T. Baron, H.-J. Lugauer, T. Litz, U. Zehnder, W. Ossau, T. Gerhard, M. Keim, G. Reuscher, and G. Landwehr, Appl. Phys. Lett. **70**, 280 (1997).

[5] V. Bousquet, E. Tournie, M. Laugt, P. Vennegues, and J. P. Faurie, Appl. Phys. Lett. **70**, 3564 (1997).

[6] D. E. Aspnes, Opt. Commun. **8**, 222 (1973).

[7] R. M. A. Azzam and N. M. Bashara, *Ellipsometry and Polarized Light* (North-Holland, Amsterdam, 1977).

[8] A. Fleszar (unpublished)

[9] R. L. Johnson, J. Barth, M. Cardona, D. Fuchs, and A. M. Bradshaw, Rev. Sci. Instrum. **60**, 2209 (1989).

[10] J. Barth, R. L. Johnson, and M. Cardona, in *Handbook of Optical Constants of Solids II*, edited by E. Palik (Academic Press, New York, 1991).

[11] T. Wethkamp, K. Wilmers, N. Esser, W. Richter, O. Ambacher, H. Angerer, G. Jungk, R. L. Johnson, and M. Cardona, Thin Solid Films **313-314**, 745 (1998).

[12] M. Cardona, J. Appl. Phys. **32**, 2151 (1961).

[13] M. Aven, D. T. F. Marple, and B. Segall, J. Appl. Phys. **32**, 2261 (1961).

[14] M. Cardona and G. Harbeke, J. Appl. Phys. **34**, 813 (1963).

[15] F. H. Pollak, *II-VI-Semiconductors*, edited by D. G. Thomas (Benjamin, New York, 1967), p. 552.

[16] J. L. Freeouf, Phys. Rev. B **7**, 3810 (1973).

[17] J. P. Walter, M. L. Cohen, Y. Petroff, and M. Balkanski, Phys. Rev. B **1**, 2661 (1970).

[18] J. R. Chelikowsky and M. L. Cohen, Phys. Rev. B **14**, 556 (1976).

[19] S. Adachi and T. Taguchi, Phys. Rev. B **43**, 9569 (1991).

[20] L. Ley, R. A. Pollak, F. R. McFeely, S. P. Kowalzyk, and D. A. Shirley, Phys. Rev. B **9**, 600 (1974).

[21] S. P. Kowalczyk, L. Ley, F. R. McFeely, and D. A. Shirley, J. Chem. Phys. **61**, 2850 (1974).

[22] W. B. Jackson and J. W. Allen, Phys. Rev. B **37**, 4618 (1988).

[23] S. Albrecht, L. Reining, R. Del Sole, and G. Onida, Phys. Rev. Lett. **80**, 4510 (1998).

[24] L. X. Benedict, E. L. Shirley, and R. B. Bohn, Phys. Rev. Lett. **80**, 4514 (1998).

[25] L. Sham and M. Schlüter, Phys. Rev. Lett. **51**, 1888 (1983).

[26] O. Zakharov, A. Rubio, X. Blase, M. L. Cohen, and S. G. Louie, Phys. Rev. B **50**, 10 780 (1994).

[27] M. Cardona, Phys. Rev. **129**, 1068 (1963).

[28] M. Cardona, N. E. Christensen, and G. Fasol, Phys. Rev. B **38**, 1806 (1988).

[29] M. Cardona and R. Haensel, Phys. Rev. B **1**, 2605 (1970).

[30] The data sets are available via electronic mail at the address katrin.wilmers@physik.tu-berlin.de